

Genome-wide profiling using single-nucleotide polymorphism arrays identifies novel chromosomal imbalances in pediatric glioblastomas

Hui-Qi Qu*, Karine Jacob*, Sarah Fatet, Bing Ge, David Barnett, Olivier Delattre, Damien Faury, Alexandre Montpetit, Lauren Solomon, Peter Hauser, Miklos Garami, Laszlo Bognar, Zoltan Hansely, Robert Mio, Jean-Pierre Farmer, Steffen Albrecht, Constantin Polychronakos, Cynthia Hawkins, and Nada Jabado

Departments of Paediatrics and Human Genetics, Montreal Children's Hospital (H.-Q.Q., C.P.); Division of Hemato-Oncology, Departments of Paediatrics and Human Genetics, Montreal Children's Hospital Research Institute (K.J., D.B., D.F., N.J.); Molecular Diagnostic Laboratory, Department of Genetics, Montreal Children's Hospital Research Institute (R.M.); Division of Neurosurgery, Montreal Children's Hospital (J.-P.F.); Department of Pathology, Montreal Children's Hospital, McGill University Health Centre, Montreal, Canada (S.A.); INSERM U 830, Institut Curie, Paris, France (S.F., O.D.); McGill University and Genome Quebec Innovation Centre, Montreal, Canada (B.G., A.M.); Division of Pathology, The Hospital for Sick Children, Toronto, Canada (L.S., C.H.); 2nd Department of Paediatrics, Faculty of Medicine, Semmelweis University, Budapest, Hungary (P.H., M.G.); Division of Neuro-Surgery, Division of Pathology, National Institute of Neurosurgery, Budapest, Hungary (L.B.); Department of Neurosurgery, Medical and Health Science Centre, University of Debrecen, Debrecen, Hungary (Z.H.)

Available data on genetic events in pediatric grade IV astrocytomas (glioblastoma [pGBM]) are scarce. This has traditionally been a major impediment in understanding the pathogenesis of this tumor and in developing ways for more effective management. Our aim is to chart DNA copy number aberrations (CNAs) and get insight into genetic pathways involved in pGBM. Using the Illumina Infinium Human-1 bead-chip-array (100K single-nucleotide polymorphisms [SNPs]), we genotyped 18 pediatric and 6 adult GBMs. Results were compared to BAC-array profiles harvested on 16 of the same pGBM, to an independent data set of 9 pediatric high-grade astrocytomas (HGAs) analyzed on Affymetrix 250K-SNP arrays, and to existing data sets on HGAs. CNAs were additionally validated by real-

time qPCR in a set of genes in pGBM. Our results identify with nonrandom clustering of CNAs in several novel, previously not reported, genomic regions, suggesting that alterations in tumor suppressors and genes involved in the regulation of RNA processing and the cell cycle are major events in the pathogenesis of pGBM. Most regions were distinct from CNAs in aGBMs and show an unexpectedly low frequency of genetic amplification and homozygous deletions and a high frequency of loss of heterozygosity for a high-grade I rapidly dividing tumor. This first, complete, high-resolution profiling of the tumor cell genome fills an important gap in studies on pGBM. It ultimately guides the mapping of oncogenic networks unique to pGBM, identification of the related therapeutic predictors and targets, and development of more effective therapies. It further shows that, despite commonalities in a few CNAs, pGBM and aGBMs are two different diseases.

Received June 11, 2008; accepted May 6, 2009.

*These authors contributed equally to the manuscript.

Corresponding Author: Constantin Polychronakos, M.D., Montreal Children's Hospital, 2300 Tupper, Montreal, Que., Canada, H3H 1P3 (constantin.polychronakos@mcgill.ca).

Keywords: pediatric high-grade astrocytomas, brain tumors, SNP arrays, LOH

Introduction

Brain tumors are the largest group of solid neoplasms in children and are currently the leading cause of cancer-related mortality and morbidity in the pediatric years. Pediatric high-grade astrocytomas (HGAs), including grade IV astrocytomas (glioblastoma [GBM]) account for 15% of all brain neoplasms in children,¹ have a dismal prognosis despite aggressive management, and have a high morbidity linked to current treatments. Although their diagnosis still relies mainly on pathology, little is known about the molecular mechanisms underlying their development.

Physical changes in the DNA copy number of particular genomic regions, manifesting as loss of heterozygosity (LOH) or epigenetic changes such as loss of imprinting, have been shown to promote cancer formation and progression. In particular, LOH has been extensively used in the discovery of various tumor suppressor genes, including *Rb1* and *p53*. A precise characterization of these genomic alterations in a given tumor may therefore increase our understanding of the oncogenic events promoting its growth and may provide more accurate means for its classification. However, most of the work done to date on nonrandom LOH in solid tumors has been based on searches for a small number of candidate loci. Comparative genomic hybridization (CGH), which identifies chromosomal segments with copy number changes (gain or loss),²⁻⁴ has an effective resolution that varies from ~20 Mb to ~100 kb and a far from optimal capacity in detecting chromosomal deletions, especially LOHs.⁵ More recently, a major breakthrough for the precise mapping of genomic aberrations in cancers has been made by the completion of the human genome sequence.⁶ Concurrently, high-density arrays for genotyping single-nucleotide polymorphisms (SNPs)^{6,7} have been made available (reviewed in Ref. 8). These arrays combine the genome-wide potential of hybridization arrays with higher-resolution (by an order of magnitude) detection of LOH, DNA copy number alterations, and other chromosomal aberrations compared to CGH.

Studies using these high-resolution arrays can be applied to unravel, with high precision, genomic imbalances in HGAs while providing an additional tool to classify these tumors. They have been used in adult HGAs (aHGAs, mainly high-resolution CGH arrays), providing more accurate tools for prognosis and the identification of therapeutic targets in this tumor.⁹⁻¹⁵ Genomic alterations involved in pHGAs are largely unknown, with only a few published studies using lower-resolution arrays.¹⁶⁻¹⁸ Moreover, pHGAs have distinct molecular profiles from aHGAs, indicating that results from adult studies cannot be applied to children.^{19,20} To identify genetic loci specifically involved in pHGAs, we analyzed 18 pediatric GBMs and 6 aHGAs using high-resolution Illumina 100K SNP arrays and an independent data set of 9 pHGAs using the Affymetrix 250K SNP arrays platform.

Materials and Methods

Sample Characteristics and Pathological Review

All samples were obtained under a protocol approved by the hospitals' institutional review boards and independently reviewed by senior pediatric neuropathologists (S.A. and C.H.) to ensure consistent classification based on contemporary guidelines from the World Health Organization. Eighteen pGBMs (average 10.3 ± 5.2 years) and 6 aGBMs (average 58.8 ± 18.2 years) were analyzed using the Illumina platform. Snap-frozen sections of areas immediately adjacent to the regions used for pathological diagnosis were provided and contained vascular tissue ranging from <10% to 30% of the full section. Normal tissue was not available for any of the samples. Tissues were obtained from the Pediatric Cooperative Human Tissue Network, the London/Ontario Tumor Bank, and from collaborators in Montreal and Toronto (Canada) and Hungary. Clinical findings of patients are provided in Table 1. Adult samples have previously been reported for gene expression analysis of pGBM.¹⁹

DNA Extraction and Hybridization

DNA from frozen tumors was extracted as described previously.¹⁶ DNA (250 ng) from 25 samples was assayed with Infinium I whole genome genotyping, according to the recommendations of the manufacturer (Illumina, San Diego, CA, USA). The Illumina Sentrix Human-1 Genotyping BeadChip covers 109,365 gene-centric SNPs over the genome with a mean intermarker distance of 26 kb (13 kb median spacing). Image intensities were extracted using Illumina's BeadScan software. Data for each BeadChip were self-normalized using information contained within the array. For Affymetrix 250K SNP chips, 250 ng of tumor DNA was processed according to the manufacturer (Affymetrix, Inc., Santa Clara, CA, USA) and data were analyzed as described elsewhere.¹⁶ Genome profiles were created using the Illumina Genome Viewer and Chromosome Browser, which allow viewing, identifying, and manually annotating the chromosomal aberrations. For the initial analysis, the output by BeadStudio software was used to interpret the nature of the aberration. These variables include the normalized intensity of hybridization, expressed as its base-2 logarithm ($\log_2 R$), and the allelic ratio, expressed as the ratio of one allele over the sum of both alleles.²¹ Visualization of copy number and LOH in normal tissues is performed by plotting the $\log_2 R$ and the allelic ratios across the genome. This algorithm, however, assumes single-lineage DNA and could not be used alone with these tumor tissue samples, which are unavoidably mixed with normal vascular tissue. Amplifications were therefore detected if there was an increase in the $\log_2 R$ value (≥ 1 , corresponding to tetraploid copy number ie ≥ 4). The SNPs with $\log_2 R \leq 2$ in tumor tissues, but with normal $\log_2 R$ in all CEU (CEPH

Table 1. Clinical characteristics of GBM samples from adult and pediatric patients analyzed using the Illumina 100K SNP array

GBM	Gender	Age at Diagnosis (Years)	Tumor Location
<i>Pediatric</i>			
P1	M	9	Infratentorial
P2	F	6	Supratentorial (frontal)
P3	F	10	Supratentorial (parietal)
P4	F	14	Supratentorial (parietal)
P5	M	14	Supratentorial (frontal)
P6	M	14	Supratentorial (temporal)
P7	F	9	Supratentorial (multilobar)
P8	M	3	Supratentorial (temporal)
P9	F	11	Supratentorial (temporal)
P10	F	13	Supratentorial (frontal)
P11	M	7	Supratentorial (thalamic)
P12	F	16	Infratentorial
P13	M	16	Infratentorial
P14	M	13	Infratentorial
P15	M	15	Infratentorial
P16	F	12	Supratentorial (parietal)
P17	F	10	Infratentorial
P18	M	13	Mixed
<i>Adult</i>			
Secondary			
A1	M	52	Supratentorial (multilobar)
A2	F	49	Supratentorial (frontal)
A3	M	67	Supratentorial (thalamic)
Primary			
A4	F	30	Supratentorial (parietal)
A5	M	70	Supratentorial (temporal)
A6	F	82	Supratentorial (frontal)

[Centre de l'Etude du Polymorphisme Humain] European) DNA samples analyzed in the HapMap project were taken as homozygous deletions.²¹ If $\log_2 R \leq 2$ in the CEU samples, the marker was discarded as a failed assay. To identify heterozygous deletions, we estimated the LOH score using the genotypes of all SNPs in a sequence window of 1 Mb, around any marker. This score is the base-10 logarithm of the ratio of the probability of observing the genotypes of all SNPs in the presence of LOH over the probability of observing the same genotype in the absence of LOH. It is based on the allele frequencies observed in the European-ancestry subjects used in the HapMap project (CEU set) and assigned to the marker in the middle of the window.²² We considered that a score of more than 10 is diagnostic of LOH. Four DNA samples from the CEU set were used as the normal control in the same assay.

BAC Arrays

The CGH-array analysis of tumor samples was performed as described previously.²³ The V5S2 genomic array uses 3913 BAC markers from across the human

genome with a mean resolution of 1 Mb. Normalization and data analyses were done with VAMP software (Bioinformatics Department, Curie Institute, Paris, France).²³ Fluorescence ratios exceeding 1.2 were considered indicative of gains of chromosomal material, whereas losses were indicated by ratios lower than 0.8.

Validation of Copy Number Changes by Quantitative Real-Time PCR

Quantitative real-time PCR was done on an ABI-Prism 7000 sequence detector (Applied Biosystems) using a SYBR Green kit (Applied Biosystems). The target locus from each tumor DNA was normalized to the reference, Line-1 as previously described.¹⁶

Statistical Analysis

To be considered causative, a somatic copy-number change must be non-random, that is, recur at the same locus in different tumors more frequently than expected by chance alone. To assess the statistical significance of the occurrence of such overlaps in different tumors, their number was compared to a distribution generated by cyclically permuting the position of the LOH regions on each chromosome of each tumor 10,000 times. The false-detection rate (FDR) was calculated as the proportion of overlaps in any given number of tumors that would be expected to occur by chance alone (see Supplementary Material, Fig. S1).

Results

Genomic Alterations Identified in BAC and in SNP Arrays in 16 pGBM Samples

We used a previously validated BAC-array platform, which has provided numerous results in tumor LOH studies,²³ and investigated the concordance of copy number aberration (CNA) detection between this platform and the Illumina 100K SNP arrays in 16 pHGAs (P1–P16; Table 1). BAC-array results validated data obtained by SNP arrays (see Supplementary Material, Table S1). However, because of the higher resolution of the SNP arrays, a higher number of alterations, left undetected by the BAC arrays, were uncovered. This is in keeping with previous findings on the higher sensitivity of SNP technology for the detection of CNAs.²⁴

CNAs in pGBM and aGBMs Detected Using Illumina SNP Arrays

Analysis of the data set of 18 pGBMs and 6 aGBMs using the Illumina SNP arrays showed that heterozygous deletions, detected as LOH, are common phenomena mostly in pGBM and were seen for each chromosome in a number of samples (Tables 1–4; see also

Table 2. CNAs identified in 18 pGBMs and aGBMs using the 100K SNP Illumina array

Tumors	No of CNAs	CNAs
P1	1	(-)22q
P2	12	(-)2q11-13, (-)9p24-21, (-)10p12-11, (-)10q, (-)14q23-32, (-)15q15-14, (-)16q, (-)17p, (+)17q21-25, del17q11, (-)19q, del21q11-21
P3	2	(-)12q24, (-)22q
P4	38	(-)2p25-11, (-)3q21-29, (-)4p16-13, (-)4p12, (+)4p13, (+)4p12, (-)4q13-35, (+)4q12, (+)5p33-15, (+)5p15-12 (-)5p15, (-)5q11-21, (-)5q31-32, (del)6q24, (-)7p, (-)7q, (+)7q31, (-)9p22-21, (+)9p24, (+)9p23-22, (+)9p21-13, (+)10p12, (-)10q11-23, (+)10q23-24, (-)10q24-26, del11q11-22, del11q22-23, (-)12q21-23, (-)13q, (-)14q, del16q23, (-)17p13-17q11, (-)18p, (-)18q, (-)19p13, (+)19p13, (-)20q, (-)22q
P5	4	(+)2p24, (+)11p, (-)11q13-25, (+)17q21-24
P6	6	(+)1q, (-)8p23, (-)9p, (+)9q, (+)21q21, (-)22q12-13
P7	23	(-)3p, (-)3q, (-)4p, (-)4q, (-)5p, (-)5q, (-)6p, (-)6q, (+)7q21, (-)8p, (-)8q, (+)9q33-34, (-)10p, (+)10p12, (-)10q, (+)13q14, (+)13q31, (+)13q33-34, (-)15q, (-)17p, (-)17q, (-)19p13, (-)22q
P8	33	(+)1q43-44, (-)2p24-23, (+)2p25, (+)2p24.3, (+)2p24.1, (+)2p23.1, (-)3p, (-)3q, (+)3q26, (-)4p, (-)4q, (-)5p, (-)5q, (-)6p, (-)6q, (+)7p11, (+)7q21, (+)7q21, (+)7q31, (+)7q33, (-)8p, (-)8q, (-)10p, (-)10q, (-)11p15, (-)11q13-23 (-)14q, (-)15q, (-)17p, (-)17q, (-)18p, (-)18q, (-)22q
P9	33	(-)1p, (-)1q, (-)2p, (-)2q, del2q21-22, (-)3p, (-)3q, (-)4q32-35, (-)5q15-35, (-)6p, (-)6q, (-)8q11-24, (-)8q24, (-)9p, del9p23, del9p21, (-)9q, (-)10p, (-)10q, (+)10q26, (-)11p, (-)11q, (-)13q, (-)14q, (-)16p, (-)16q, (-)17p, (-)17q, (-)18p, (-)18q, (-)20p, (-)20q, (-)21q
P10	17	(-)2p, (-)3q12-27, (+)3q26-29, (-)4q31, (+)7p, (+)7q, (-)8p21-12, (-)8p12-11, (-)9p21-13, 9q31-33, (-)10p, del 10q21-22, (-)10q25-26, (-)11q22-24, (-)14q31-32, (-)17p13, (-)19q13
P11	4	(-)1p, (-)6q12-13, (+)6q14, (-)6q14-27
P12	4	(-)10q21-26, (-)15q12-26, (-)16p, (+)17p13
P13	15	del1q24-31, (+)5p15, (+)7p22, (+)7p21, (+)7p21, (-)9p24-22, (-)9p21, (-)10q23-26, (+)10q22, (+)10q23, (-)16q, (-)17p, (-)18q12-23, (-)20p, (-)21q
P14	1	(-)22q
P14	4	(+)2p24, (+)4q12, (+)7p, (+)7q
P16	1	(+)9p21-13
P17	1	(+)7q11
P18	0	
A1	10	(+)3p11-12, (-)3p26-24, (-)3q27-28, (-)3q29, (-)9p, del9p22-21, (-)9q12-21, (-)10p, (-)10q, (-)22q12-13
A2	14	(-)3p26, (-)9p24-21, (-)9p21, (-)9p13, (-)9q22, (-)11p15, 12p13-12, (-)13q12-21, del 14q23, del14q24, (-)10p, (-)10q, (-)17p13, (-)19q13, (-)21q, (-)22q13
A3	3	(-)4q13-35, (-)9p24-21
A4	4	(+)7p11-14; del 9p22-21, (-)10q, (+)12q13-15, (-)19p12
A5	9	(-)5q, (-)7q11-21, (-)11p15-11, (-)12p, (-)13q, (-)14q, (-)17p13-11, (-)18p11, (-)21q22
A6	2	(+)7p14-15, (+)7p11-15, (-)10q

A, adult glioblastoma; P, pediatric glioblastoma. (-) indicates an LOH; (+) indicates an amplification or gain; "del" indicates a homozygous deletion.

Supplementary Material, Table S1). Despite common LOH regions between pGBM and aGBM such as 9p24.3-9p13.1 and 17p13.3, there was little concordance between the CNAs detected in both settings, with most LOHs (Tables 3 and 4), amplifications (Table 5), and homozygous deletions (Table 6) found in children being different from the ones encountered in adults (Tables 2–6). Unsupervised hierarchical clustering analysis, using as input data regions with CNAs in at least one sample, clustered the aGBM samples separately from most pGBMs and the normal brain, confirming the presence of distinct molecular imbalances specific to pGBM.¹⁹ Interestingly, it also separated primary from secondary aGBMs (Fig. 1).

Analysis of Recurrent Regional LOH in GBMs

Several overlapping regions of LOH in tumors were identified in pGBM samples (Tables 3 and 4). By permutation analysis, the 95% confidence interval of the FDR for seven tumor-overlaps is 0–0.096, which makes it unlikely that more than one of these overlaps is the result of chance alone (see Supplementary Material, Fig. S1). Some of these LOHs found in more than seven samples have been previously described, but most are novel (Tables 2–4). The highest LOH frequency peak in pGBM was from a 103-kb cluster located in Chr15q15 (10/18) (Tables 3 and 4). Novel genes, including protein p53 binding protein 1 (*TP53BP1*) and Cyclin

Table 3. LOH analysis showing distinct imbalances between pGBM and aGBM

Cytogenetic Band	Locus (Mb)				Minimal Region	Genes	Number of Tumors	Known or Novel	Interesting Genes		
	Start SNP	Position	End SNP	Position							
<i>LOH regions in 19 pGBMs</i>											
2p25.3-2p11.2	rs876724	104974	rs4832054	86970238	2p24.1-2p23.1	100	4	Novel			
3q12.1-3q29	rs7614366	100979041	rs7374380	199195232	3q21.1-3q26	361	5	Novel			
4q13.1-4q35.2	rs1449043	59562234	rs1317423	191081281	4q32.3-4q35.2	137	5	Novel			
5q11.1-5q21.3	rs4865676	49610934	rs7701086	109419588	5q11.1-5q21.3	348	4	Novel			
6q12-6q27	rs9363741	68085762	rs2021899	170823609	6q12-6q27	630	4	Novel			
8p23.3-8p11.21	rs888580	204809	rs907561	40930754	8p23.3-8p11.21	373	4	Novel			
9p24.3-9p13.1 ^a	rs493348	202421	rs7848575	38708308	9p24.3-9p22.1	92	5	Known	ELAVL2	CDKN2A	CDKN2B
10p					10p12.31-10p11.1	133	5	Novel			
10q22.1-10q26.3	rs10762360	71729512	rs2803990	134410330	10q22.1	1	7	Novel	CBARA1		
11q13.2-11q25	rs3133269	67560732	rs4300405	133977871	11q22.1-11q23.1	107	4	Novel			
14q23.3-14q32.33	rs1290900	66770921	rs7492357	105033704	14q31.3-14q32.31	189	5	Novel			
15q15.1-15q23	rs2289218	38853018	rs10220851	66092261	15q15.2-15q15.3	13	10	Novel	CCNDBP1	TP53BP1	H76p
16q					16q		4	Known			
17p13-17p11.2	rs2750007	623976	rs4924750	18201478	17p13.3 ^a	3	7	Novel	SMYD4	RPA1	
					17p13.1	2	7	Novel	CLEC10A	ASGR2	
					17p13.1	79	7	Novel	GPS2		
18q12.2-18q23	rs1484095	33971576	rs4798947	76064957	18q23	19	4	Novel	KCNG2		
22q11.1-22q13	rs3788277	16054103	rs6520165	49144461	22q12.2	1	7	Novel	NF2		
					22q12.3	7	7	Novel	KCTD17		
					22q13.1	18	7	Novel	RAC2	CDC42EP1	
					22q13.1	9	7	Novel	LOC400927	TPTE, PTEN homologs	
<i>LOH regions in 6 aGBMs</i>											
3p26.3-3p24.2	rs6803398	982443	rs892940	24513842	3p26.3	4	2	Novel	CHL1		
9p24.3-9p13.1 ^a	rs6477419	979943	rs7036799	38747881	9p24.3-9p21.1	146	3	Known	ELAVL2	CDKN2A	CDKN2B
11p15.5-11p11.2	rs2280544	194062	rs6485999	49615562	11p15.4	1	3	Known			
17p13.3-17p11.2	rs4985615	172350	rs9783820	18601046	17p13.3 ^a	21	2	Novel	TUSC5		
22q12.2-22q13.33	rs7289095	28983276	rs1001469	49428897	22q13.2-22q13.3	122	2	Known			

^aCommon alterations between pGBM and aGBM.

Table 4. Identification of statistically overrepresented gene ontologies (GOs) in the genes harbored in LOH regions analyzed using the Gostat tool (<http://gostat.wehi.edu.au/cgi-bin/goStat.pl>)

Gene Ontology Term	<i>p</i>	Number of Genes	Total
Negative regulation of biological process	3.80E-11	119	1187
Cell-cycle process	5.08E-11	89	809
System development	5.83E-11	149	1623
Negative regulation of cellular process	2.40E-10	109	1095
Cellular developmental process	3.22E-10	198	2389
Cell differentiation	3.22E-10	198	2389
Regulation of cell proliferation	3.21E-09	55	446
Transcription from RNA polymerase II promoter	4.01E-09	71	642
Regulation of cellular process	6.90E-09	393	5660
Organ development	6.90E-09	111	1183
Positive regulation of cellular process	3.34E-08	89	905
Cell development	5.44E-08	155	1865
Regulation of cell cycle	5.71E-08	65	599
Regulation of progression through cell cycle	1.09E-07	64	594
Positive regulation of biological process	3.01E-07	104	1152
Defense response to bacterium	2.14E-06	18	99
Negative regulation of cell proliferation	9.98E-06	29	216
Cell death	1.12E-05	79	862
Death	1.12E-05	79	862
Protein kinase cascade	1.12E-05	42	370
Apoptosis	1.12E-05	75	807
Response to bacterium	1.43E-05	18	107
Programmed cell death	1.48E-05	75	813
Enzyme-linked receptor protein signaling pathway	1.57E-05	35	290
Cell migration	1.64E-05	30	233

The complete database of annotated human genes was used as a control set. Results were filtered to include only GOs with a minimum path length of 5 and that fall under the biological process segment of the GO hierarchy.

D-type binding-protein 1 (*CCNDBP1*), and two potential tumor suppressor genes that regulate the *p53* and the *Rb* pathways are within this LOH peak.

Analysis of Regional Chromosomal Amplification and Homozygous Deletions in GBMs

Only a small number of amplifications (defined as 4 copies or more) and homozygous deletions were found in the pGBM samples. These were mainly in regions close to the centromeres of Chrs 5, 7, 11, 19, and 20, where typically no genes are found (Table 3). In contrast, chromosomal amplifications were more frequent in aGBMs (Tables 1 and 5). For example, all aGBMs had amplification of 4p16, 5p11, 11q11, and

20p11.2, and five of six had amplification in 8p23 and 19p12-13.3. Further, as expected and previously shown, epidermal growth factor receptor (*EGFR*) maps to the largest SNP cluster of amplification in Chr7p12 in two-thirds of the primary aGBMs included in this study (Table 5).^{25,26} In pGBM, a previously described amplification of 7p12 including *EGFR* was observed with a similar incidence to what is reported in the literature (2 of 18; 10.5%). However, a new amplification in 7q21-22 including *CDK6* (Cyclin D Kinase 6) was seen in 5 of 18 pGBMs. All tumors were supratentorial. Interestingly, the latter is a known copy number variant with a seemingly higher incidence in pGBM than in the general population (5 of 18 versus 7 of 270; 26% versus 3%, *p* < 0.001, Fisher exact test). For regional homozygous chromosomal deletion, the most significant finding was the deletion of an SNP cluster in aGBMs containing interferon genes (*IFNB1*, *IFNW1*, *IFNA21*) that are important in the induction of *p53* gene expression (Table 6).²⁷ No homozygous deletions were observed in pGBM.

Validation of CNAs Identified in This Study

In the absence of control DNA from the same individual allowing confirmation that the CNAs we observed are tumor-derived and not a normal variant, we cross-referenced our data with the Database of Genomic Variants and the CEU study.^{28,29} We additionally cross-referenced our data for the most relevant CNAs with data from a set of 1,363 control DNA analyzed with the Illumina Human-Hap 300K platform.³⁰ This allowed us to identify some previously reported regions of common structural polymorphisms in the general population, further validating the other regions as tumor-specific LOHs (Tables 2-6; see also Supplementary Material, Tables S1 and S2). We also compared our data with other available genotyping studies on pHGAs¹⁶⁻¹⁸ and on aHGAs^{9,31,32} as the number of adult cases used for comparison in this study is too few to make a meaningful conclusion. We also compared our data set to two publicly available 100K SNP array data sets on aHGAs (NCBI GEO DataSets as GSE9635 and GSE6109 Records).^{13,33} Cross-referencing our results with these data sets on aHGAs showed several commonalities with previously published studies, mainly for the adult patients included in our study (Pearson correlation, *r*: 0.83 and Tables 1-6; see also Supplementary Material, Table S1); however, only few previously published CNAs were common with pGBM (Pearson correlation, *r*: 0.21). We further validated the data set against an independent data set of 9 pGBMs analyzed using another SNP platform, the Affymetrix 250K SNP array that interrogates more than 200,000 loci and has a similar average resolution of 15 kb,³⁴ and obtained concordant results for several CNAs, further validating data obtained using the Illumina SNP arrays (see Supplementary Material, Fig. S2).

We also arbitrarily chose a set of genes involved in regions identified as homozygous deletions, LOH, or

Table 5. Amplifications in pGBM and aGBM

Cytogenetic Band	Locus (Mb)				Minimal region	Genes	Number of Tumors	Known or Novel	Interesting Genes
	Start SNP	Position	End SNP	Position					
<i>Amplifications in pGBM</i>									
1q					1q43-1q44	26	2	Novel	AKT3
2p24.3	rs12616227	14424553	rs300168	17884078	2p24.3	15	3	Known	MYCN
3q26-3q29	rs7638716	174896221	rs6770002	199198093	3q26.31-3q26.33	34	2	Novel	PIK3CA, NGL1
4q12	rs11734039	54105356	rs7692791	55821167	4q12	11	2	Known	PDGFRa, KIT
5p33-5p15	rs4956990	236134	rs2578553	5502367	5p15.33-5p15.2	62	2	Novel	TPPP
7p22.3-7p11.2 ^a	rs7786069	160449	rs4947882	54032344	7p22.3-7p11.2	417	2	Known	EGFR
7q11.21-7q33 ^b	rs2198391	61491258	rs3735019	137020053	7q21.13-7q21.3	23	5	Novel	CDK6
7q11.21-7q33	rs2198391	61491258	rs3735019	137020053	7q31.2-7q33	163	4	Novel	
9p24.3-9p13	rs999924	1322257	rs2799738	38468670	9p13.3-9p13.1	122	3	Novel	
9q					9q33.1-9q34.3	265	2	Novel	
10p12.31-10p12	rs1055340	16595534	rs751006	26145481	10p12.2-10p12.1	3	2	Novel	OTUD1
10q22.2-10q26.3	rs4746308	76999278	rs2515641	135240243	10q22.2-10q26.3	516	3	Novel	PTEN
17q21-17q25.3	rs8074034	44287297	rs599314	78321361	17q21.33-17q22	73	2	Novel	
<i>Amplifications in aGBMs</i>									
3p12.3-3p11.2	rs4258921	81083700	rs1521800	90084278	3p12.3-3p11.2	21	1	Novel	EPHA3
7p15.2-7p11.1	rs10259620	26975529	rs6974091	57689510	7p15.2-7p14.1	38	2	Novel	CREB5
7p12 ^a	rs1454520	54455112	rs7796351	55230615	7p11	6	2	Known	EGFR
12q14.3-12q15	rs1797404	64866345	rs7973221	69380480	12q14.3-12q15	41	1	Novel	NGFR

Seventeen (94.4%) of the 18 pediatric patients and all the 6 adult patients have at least one amplification. All the samples have at least 2 loci with amplification or homozygous deletion.

^aCommon alterations between pGBM and aGBM.

^bKnown CNA with a much higher incidence than the one found in the normal population.

DNA amplification in our data set and validated these CNAs using quantitative real-time (qRT)-PCR on DNA extracted from the same tumors (Tables 5 and 6). *ELAVL2* (embryonic lethal, abnormal vision, *Drosophila*-like 2), a gene located on 9p21, was within a region of LOH in 5 of 18 pGBMs and potentially deleted in 1 of 18. We confirmed these results using qRT-PCR (Table 7). Chromosomal amplification in pGBMs on 7q21-22, which contains *CDK6*, was identified in 5 of 18 tumors. *CDK6* amplification was also confirmed using qRT-PCR (Table 7).

Discussion

Understanding the molecular pathogenesis of pHGAs requires a detailed cataloguing of all the genetic lesions in the somatic lineage of this cancer. This study includes the largest cohort of pGBMs analyzed for genomic imbalances in tumor DNA and is the first to use high-resolution SNP arrays. While further confirming that aGBM and pGBM are genetically distinct cancers, we provide a comprehensive whole-genome map of CNAs for pGBM and identify, within regions of CNAs, altered genes and pathways for further analysis (Tables 1–7).

Our data show findings in common with available array-based genomic studies on pGBM, including *ELAVL2*, *CDKN2A*, and *CDKN2B* deletions that have been reported in both pGBM and aGBM,

supporting the validity of our data set. However, previous studies on pHGAs used arrays that had a lower resolution of at least one log than the 100K and 250K arrays used in this study.¹⁶ In these former studies, as for BAC arrays, this resulted in a vast number of genetic abnormalities going undetected. We uncover herein several previously unidentified CNAs specific to pediatric tumors that help provide insight into molecular pathways involved in the genesis of pGBM. These CNAs include LOH in 15q15.1-15q23 and 17p13-17p11.2 and amplification of 7q21-22 and 1q43-44. Even if some CNAs are common to the pediatric and adult setting, their overall incidence will differ whether they occur in children or in adults. When we reviewed published data sets on aHGAs, commonalities with our findings on pGBM included LOH of 22q17p and 9p, whereas LOH of 3p21 and 10q21 and amplification of 7q, 2p, 9p, and 10q seemed specific to pGBM (see Supplementary Material, Table S2). As an added example, amplification of 7p12 including *EGFR* is a frequent event in primary aGBMs (~45%).^{9,35} We and others^{16,36} show amplification of 7p12 including *EGFR* in only rare cases of pediatric GBMs (less than 10%). Conversely, amplification of 7q21-22 including *CDK6* is a rare event in aHGAs (one case report), whereas it was present in 5 of 18 pGBMs. In addition, as a consequence of the higher resolution of the arrays we used, the genetic interval subject to alteration in tumors will differ in pediatric and adult samples in many cases. For example, 10q LOH/deletion will

Table 6. Homozygous deletions in pGBM and aGBM

Cytogenetic Band	Locus (Mb)		Minimal Region		Genes	Number of Tumors	Known or Novel	Interesting Genes	
	Start SNP	Position	End SNP	Position					
<i>Deletions in pGBM</i>									
1q24.2-1q31.1	rs2901029	165831827	rs1011726	187652124	1q24.2-1q31.1	195	1	Novel	FASLG
2q21.1-2q22.2	rs1918615	140631475	rs1465839	143468685	2q21.1-2q22.2	3	1	Novel	LOC730114
5q14.2-5q22.1	rs2656989	82226475	rs6881837	111305383	5q14.2-5q22.1	111	1	Novel	
6q24.3	rs1832378	145733157	rs1039085	147677240	6q24.3	13	1	Novel	RAB32
9p23	rs419387	10050049	rs10809546	11642121	9p23	3	1	Novel	
9p21.2 ^a	rs1475660	20746547	rs1197944	27991944	9p21.2	48	1	Known	ELAVL2, CDKN2A-2B
10q21.3-10q22.1	rs747942	71006472	rs10823922	73852923	10q21.3-10q22.1	35	1	Novel	CBARA1
11q11-11q22.3	rs9666583	54865587	rs7112835	108318814	11q11-11q22.3	858	1	Novel	
11q22.3-11q23.1	rs7112835	108318814	rs1293344	111542594	11q22.3-11q23.1	37	1	Novel	ARHGAP20
16q23.2-16q23.3	rs7204972	79379066	rs9922131	81700946	16q23.2-16q23.3	16	1	Novel	PLCG2
17q11.2	rs1061346	26138355	rs9915569	27490232	17q11.2	24	1	Novel	OMG
18q23	rs2196736	74449768	rs4798947	76064957	18q23	19	1	Novel	KNCG2
21q11.2-21q21.3	rs2742158	13560787	rs3737413	26270243	21q11.2-21q21.3	64	1	Novel	BIC
<i>Deletions in aGBMs</i>									
9p21.3	rs1556475	20811287	rs2939	21156004	9p21	5	3	Novel	INFB1, INFA21
14q23.2	rs1695770	64284919	rs8015408	66216433	14q23.2	19	1	Novel	MAX, YBX1P1
14q24.1-14q24.2	rs8016781	68963945	rs6574074	71945439	14q24.1-14q24.2	26	1	Novel	SIPA1L1

Fifteen (83.3%) of the 18 pediatric patients and all the 6 adult patients have at least one homozygous deletion. All the samples have at least 2 loci with amplification or homozygous deletion. Homozygous deletion in 10q including PTEN was found in 4 of 6 adult tumors and is not included as it is a known alteration.

^aCommon alterations between pGBM and aGBM.

Table 7. Validation of Illumina Infinium 1 SNP-array data using qRT-PCR on selected genes

	Illumina data	Normalized ratio	Normalized STD
<i>CDK6</i>			
P1	Normal copy number	1.24	0.52
P2	Amplification	114.45	7.63
P3	Amplification	42.55	7.26
P5	Amplification	3.80	0.86
P7	Normal copy number	1.34	0.36
P11	Amplification	2.63	0.38
P13	Normal copy number	1.27	0.28
P15	Normal copy number	1.20	0.31
P16	Amplification	7.82	0.27
<i>ELAVL2</i>			
P13	LOH	0.40	0.13
P15	LOH	0.50	0.07
P12	LOH	0.42	0.14
P11	Homozygous deletion	0.19	0.04
P1	LOH	0.46	0.11
P7	LOH	0.48	0.16
P2	Normal copy number	1.20	0.17
P4	Normal copy number	0.80	0.23
P6	Normal copy number	1.10	0.32

To validate results we obtained following the analysis of data from SNP arrays, we selected previously identified genes in high-grade astrocytomas that were included in regions showing chromosomal amplification (*CDK6*, amplification of Ch 7q21 in 5 tumors P2–P3–P5–P11–P16) or LOH or homozygous deletion (*ELAVL2*, LOH in P1–P7–P13–P15–P12, complete deletion in P11) and performed qRT-PCR on DNA extracted from the same tumors and from other tumors included in this study and showing no copy number change for these regions. Normalized ratio obtained using qRT-PCR was interpreted as follows: <0.2 homozygous deletion; $0.4 < X < 0.6$ LOH; >2 amplification. Pediatric high-grade astrocytomas were numbered from 1 to 18 for clarity issues with the suffix P for pediatric. *CDK6*, cyclin D kinase 6; *ELAVL2*, embryonic lethal, abnormal vision, drosophila-like 2; STD, standard deviation.

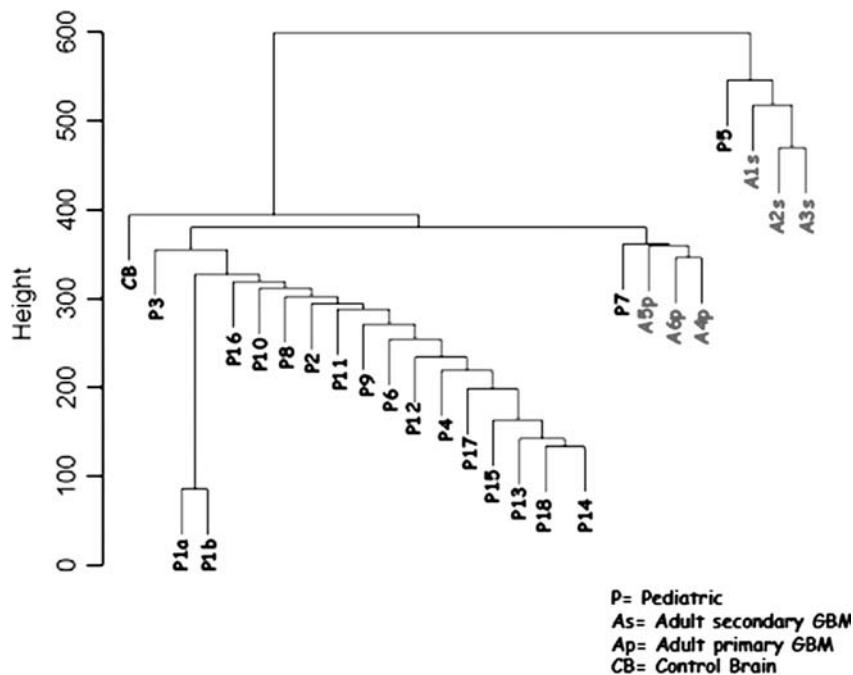


Fig. 1. Unsupervised hierarchical clustering of 24 GBMs (18 pediatric and 6 adult) and 1 control normal brain (CB). We used statistically significant CNAs present in at least one sample as data input (Welsh *t*-test, $p < 0.001$) and separated our data set accordingly. Pediatric (P) samples clustered separately from adult samples (A) and from the CB. DNA from one pediatric sample P1 was extracted from two separate parts of the same tissue sample. DNA from both extractions was independently subjected to whole-genome amplification prior to analysis on the 100K SNP array platform. P1a and P1b clustered similarly showing the reproducibility of the analysis of genome profiling. Primary adult glioblastoma (Ap) clustered separately from secondary adult glioblastoma (As).

include the PTEN gene (10q23.31) in adults whereas the genetic interval will be different in children and LOH on 10q will not include it (10q21.3-10q22.1).

Cell-cycle abnormalities, including alterations of the *p53* and the *RB1* pathways, play an important role in the genesis of HGAs, including pHGAs.^{20,26} As shown in the analysis of genes included in the CNA regions (Tables 3–6) and by the gene ontology analysis (Table 4), genes associated with the cell-cycle checkpoints and genes involved in the regulation of cell-cycle and cell-death pathways are the major targets of LOHs in pGBM. For example, we identified recurrent LOHs in several tumors that encompass several genes including *H76p*, *TP53BP1*, and *CCNDBP1* on 15p (Table 3). *H76p* is associated with the γ -tubulin complexes and may participate in the nucleation process.³⁷ *TP53BP1* is a conserved checkpoint protein with properties of a DNA double-strand break sensor. It binds to the central domain of *p53*, enhancing transactivation, and its deletion may play an important role by impairing function of tumor protein *p53* (*TP53*).³⁸ *CCNDBP1* is a helix–loop–helix leucine zipper protein, recently identified as a novel tumor suppressor in epithelial cancers, showing LOH and/or deletions on Chr15.³⁹ It decreases the levels of Cyclin D expression, reducing the phosphorylation of *RB1*, thus regulating the *RB1* pathway and cell growth.³⁹

The rare gene containing regions showing genomic amplification in pGBM included 7q21-22 in 5 pGBMs (Table 5). This region is interesting from two standpoints. It includes *CDK6*, which encodes for a kinase also regulating the *RB1* pathway. Amplification of *CDK6* in this subset of pGBM was validated by qRT-PCR (Table 7) and has not been previously reported in pHGAs. In aHGAs, amplification of *CDK6* has been reported in only one patient, whereas its overexpression, without genetic amplification, is more common (~40%). Secondly, a CNA found with statistically higher frequency in a given tumor is likely a germline predisposition to the tumor. 7q21-22 seems to be amplified in a small percentage of the normal population, and the higher incidence of its amplification in pGBM, when further confirmed, may indicate an

association of a common variant with susceptibility to these tumors (Table 5).

Little is known on the genetics of pGBM and our study fills an important gap in understanding this pediatric brain tumor. Moreover, the considerable wealth of information on the molecular genetics of aHGA is often projected onto the pediatric population without critical comparison between these two different disease contexts. Our data document how profound these differences are. We propose that analyses such as the one presented in this study may ultimately guide mapping of oncogenic signaling networks unique to pGBM, identification of the related therapeutic predictors and targets, and development of more effective therapies. Alteration of copy number for genes involved in *p53* and the *RB* pathways including, for example, amplification of *CDK6*, or LOH of *CCNDBP1* or *TP53BP1*, are some of the interesting findings unraveled in our data set that will help shed light on the unique molecular pathogenesis of this disease, providing hope of developing new therapeutic strategies to improve survival in a devastating cancer.

Supplementary Material

Supplementary material is available at *Neuro-Oncology Journal* online.

Acknowledgments

This work was supported by the Canadian Institutes of Health Research, the Cole Foundation, One Day at a Time, and the Vinchiaturese Association (N.J.), the Hungarian Scientific Research Fund (OTKA) Contract No. T-04639, and the National Research and Development Fund (NKFP) Contract No. 1A/002/2004 (P.H., M.G., L.B., and Z.H.). H.Q. and K.J. are the recipients of a fellowship and a studentship, respectively, from the Canadian Institutes of Health Research. N.J. is the recipient of a Chercheur Boursier Award from Fonds de la Recherche en Sante du Quebec.

Conflict of interest statement. None declared.

References

1. Broniscer A. Past, present, and future strategies in the treatment of high-grade glioma in children. *Cancer Invest.* 2006;24:77–81.
2. Vissers LE, Veltman JA, van Kessel AG, et al. Identification of disease genes by whole genome CGH arrays. *Hum Mol Genet.* 2005;14(2):R215–R223.
3. Pinkel D, Albertson DG. Comparative genomic hybridization. *Annu Rev Genomics Hum Genet.* 2005;6:331–354.
4. He M, Rosen J, Mangiameli D, et al. Cancer development and progression. *Adv Exp Med Biol.* 2007;593:117–133.
5. Thomas R, Scott A, Langford CF, et al. Construction of a 2-Mb resolution BAC microarray for CGH analysis of canine tumors. *Genome Res.* 2005;15:1831–1837.
6. Altshuler D, Brooks LD, Chakravarti A, et al. A haplotype map of the human genome. *Nature.* 2005;437:1299–1320.
7. Gunderson KL, Steemers FJ, Lee G, et al. A genome-wide scalable SNP genotyping assay using microarray technology. *Nat Genet.* 2005;37:549–554.
8. Dutt A, Beroukhi R. Single-nucleotide polymorphism array analysis of cancer. *Curr Opin Oncol.* 2007;19:43–49.
9. Maher EA, Brennan C, Wen PY, et al. Marked genomic differences characterize primary and secondary glioblastoma subtypes and identify two distinct molecular and clinical secondary glioblastoma entities. *Cancer Res.* 2006;66:11502–11513.
10. Nigro JM, Misra A, Zhang L, et al. Integrated array-comparative genomic hybridization and expression array profiles identify clinically relevant molecular subtypes of glioblastoma. *Cancer Res.* 2005;65:1678–1686.

11. Rich JN, Hans C, Jones B, et al. Gene expression profiling and genetic markers in glioblastoma survival. *Cancer Res.* 2005;65:4051–4058.
12. Phillips HS, Kharbanda S, Chen R, et al. Molecular subclasses of high-grade glioma predict prognosis, delineate a pattern of disease progression, and resemble stages in neurogenesis. *Cancer Cell.* 2006;9:157–173.
13. Kotliarov Y, Steed ME, Christopher N, et al. High-resolution global genomic survey of 178 gliomas reveals novel regions of copy number alteration and allelic imbalances. *Cancer Res.* 2006;66:9428–9436.
14. Horvath S, Zhang B, Carlson M, et al. Analysis of oncogenic signaling networks in glioblastoma identifies ASPM as a molecular target. *Proc Natl Acad Sci USA.*, 2006;103:17402–17407.
15. McLendon R, Friedman A, Bigner D, et al. Comprehensive genomic characterization defines human glioblastoma genes and core pathways. *Nature.* 2008;455:1061–1068.
16. Wong KK, Tsang YT, Chang YM, et al. Genome-wide allelic imbalance analysis of pediatric gliomas by single nucleotide polymorphic allele array. *Cancer Res.* 2006;66:11172–11178.
17. Warr T, Ward S, Burrows J, et al. Identification of extensive genomic loss and gain by comparative genomic hybridisation in malignant astrocytoma in children and young adults. *Genes Chromosomes Cancer.* 2001;31:15–22.
18. Rickert CH, Strater R, Kaatsch P, et al. Pediatric high-grade astrocytomas show chromosomal imbalances distinct from adult cases. *Am J Pathol.* 2001;158:1525–1532.
19. Faury D, Nantel A, Dunn SE, et al. Molecular profiling identifies prognostic subgroups of pediatric glioblastoma and shows increased YB-1 expression in tumors. *J Clin Oncol.* 2007;25:1196–1208.
20. Rood BR, Macdonald TJ. Pediatric high-grade glioma: molecular genetic clues for innovative therapeutic approaches. *J Neurooncol.* 2005;75(3):267–272.
21. Steemers FJ, Gunderson KL. Illumina, Inc. *Pharmacogenomics.* 2005;6:777–782.
22. Peiffer DA, Le JM, Steemers FJ, et al. High-resolution genomic profiling of chromosomal aberrations using Infinium whole-genome genotyping. *Genome Res.* 2006;16:1136–1148.
23. La Rosa P, Viara E, Hupe P, et al. VAMP: visualization and analysis of array-CGH, transcriptome and other molecular profiles. *Bioinformatics.* 2006;22:2066–2073.
24. Greshock J, Feng B, Nogueira C, et al. A comparison of DNA copy number profiling platforms. *Cancer Res.* 2007;67:10173–10180.
25. Wong AJ, Bigner SH, Bigner DD, et al. Increased expression of the epidermal growth factor receptor gene in malignant gliomas is invariably associated with gene amplification. *Proc Natl Acad Sci USA.* 1987;84:6899–6903.
26. Zhu Y, Parada LF. The molecular and genetic basis of neurological tumours. *Nat Rev Cancer.* 2002;2:616–626.
27. Takaoka A, Hayakawa S, Yanai H, et al. Integration of interferon-alpha/beta signalling to p53 responses in tumour suppression and antiviral defence. *Nature.* 2003;424:516–523.
28. Conrad DF, Andrews TD, Carter NP, et al. A high-resolution survey of deletion polymorphism in the human genome. *Nat Genet.* 2006;38:75–81.
29. Hinds DA, Kloek AP, Jen M, et al. Common deletions and SNPs are in linkage disequilibrium in the human genome. *Nat Genet.* 2006;38:82–85.
30. Hakonarson H, Grant SF, Bradfield JP, et al. A genome-wide association study identifies KIAA0350 as a type 1 diabetes gene. *Nature.* 2007;448:591–594.
31. Bredel M, Bredel C, Juric D, et al. High-resolution genome-wide mapping of genetic alterations in human glial brain tumors. *Cancer Res.* 2005;65:4088–4096.
32. Liu F, Park PJ, Lai W, et al. A genome-wide screen reveals functional gene clusters in the cancer genome and identifies EphA2 as a mitogen in glioblastoma. *Cancer Res.* 2006;66:10815–10823.
33. Beroukhi R, Getz G, Nghiemphu L, et al. Assessing the significance of chromosomal aberrations in cancer: methodology and application to glioma. *Proc Natl Acad Sci USA.* 2007;104:20007–20012.
34. Mullighan CG, Goorha S, Radtke I, et al. Genome-wide analysis of genetic alterations in acute lymphoblastic leukaemia. *Nature.* 2007;446:758–764.
35. Ohgaki H, Dessen P, Jourde B, et al. Genetic pathways to glioblastoma: a population-based study. *Cancer Res.* 2004;64:6892–6899.
36. Pollack IF, Hamilton RL, James CD, et al. Rarity of PTEN deletions and EGFR amplification in malignant gliomas of childhood: results from the Children's Cancer Group 945 cohort. *J Neurosurg.* 2006;105:418–424.
37. Fava F, Raynaud-Messina B, Leung-Tack J, et al. Human 76p: a new member of the gamma-tubulin-associated protein family. *J Cell Biol.* 1999;147:857–868.
38. Wang B, Matsuoka S, Carpenter PB, et al. 53BP1, a mediator of the DNA damage checkpoint. *Science.* 2002;298:1435–1438.
39. Ma W, Stafford LJ, Li D, et al. GCIP/CCNDBP1, a helix–loop–helix protein, suppresses tumorigenesis. *J Cell Biochem.* 2007;100:1376–1386.